A NOVEL DUAL-BAND PASSBAND FILTER WITH CONTROLLABLE CENTER FREQUENCIES AND BANDWIDTHS

Zhi-Peng Li[*], Tao Su, Yong-Liang Zhang, and Chang-Hong Liang

Key Laboratory of Science and Technology on Antennas and Microwaves, Xidian University, Xi'an, Shaanxi 710071, People's Republic of China

Abstract—A high-order dual-band bandpass filter using novel combined stub-loaded resonators (CSLRs) is presented in this paper. The key merits of the filter configuration are that the center frequency and also the bandwidth of each passband can be controlled conveniently. Moreover, it can build the high-order dual-band bandpass filters using the proposed resonators because of the sufficient coupling through the four symmetric stubs. A fifth-order dual-band bandpass filter designed at 2.5/3.5 GHz was built and tested. The measurement and simulation results agree very well, demonstrating the validity of the method.

1. INTRODUCTION

Recently, dual-band technology has been gaining much attention in modern mobile and wireless communication systems. To meet various application requirements, dual-band filters have been proposed and exploited extensively as a key circuit block in dual-band wireless communication systems. Many different methods, especially multi-mode resonators like step-impedance resonators (SIRs), stub-loaded resonators (SLRs) with controllable frequency response have been widely used to design of dual-band BPFs [1–19]. In [1], the dual-band filters were designed using centrally loaded resonators, where only the second-order filters were considered. In [2–5], the authors presented a dual-band filter with independently controlled bandwidths, but can hardly extend to high-order filters. Additionally, several dual-band

filters were designed as high-order BPFs described in [6, 7], but the bandwidths of the two passbands cannot be controlled independently. To get more flexibility, the multi-stub loaded resonator configuration is proposed [8], which can easily extend to high-order filters, but a fly in the ointment is only the second bandwidth can be controlled independently. And some other design procedures about dual-band filter have been discussed in paper [9–19].

Although design methodologies of dual-band have been discussed in many papers, few of them can extend to high-order BPFs, not to mention the controllable of bandwidth and center frequency of the two passbands independently. In this letter, combined stub-loaded resonators (CSLRs), which contain four open stubs (two top stubs and two bottom stubs), are proposed to develop dual-band BPF with controllable center frequencies and bandwidths. The resonant frequencies of the proposed resonator can be conveniently controlled by tuning the stub parameters. Moreover, the required coupling strength between the adjacent resonators can be obtained by appropriately adjusting the position of four symmetric stubs. So, it is possible to build the high-order dual-band filters using the proposed resonators. To verify the design method, a fifth-order BPF is designed, fabricated, and tested.

2. DETERMINE THE RESONANCE BEHAVIORS OF COMBINED STUB LOADED RESONATOR

The basic structure of a CSLR is shown in Figure 1. It is carefully combined by a via that connects the two SLRs to the ground plane. The input admittance of a single SLR can be obtained as:

$$Y_{in} = jY \frac{2 \tan \theta_1^i \tan \theta_2^i - 1}{\tan \theta_1^i - \tan \theta_2^i - \tan \theta_1^i \tan^2 \theta_2^i} \quad i = 1, 2 \qquad (1)$$

Thus, the resonant condition can be expressed as:

$$2 \tan \theta_1^i \tan \theta_2^i = 1 \qquad (2)$$

It can be observed from Formula (2) that the resonant condition of SLR is the same as the resonant condition of $\lambda_g/4$ SIR. Moreover, an advantage is that CSLR is more convenient to realize high order filter than SIR. It will be described in the following sections.

It should be noticed that the two resonant conditions need not be satisfied simultaneously. So, the two resonant frequencies can be controlled independently. As shown in Figure 2, the first passband frequency can be shifted with a wide range by changing the stub length θ_1^1, while the second passband frequency is fixed. Besides that,
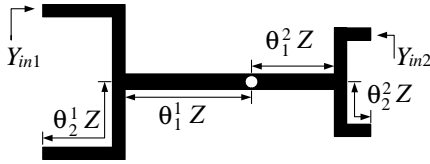
Figure 1. Structure of the CSLR.
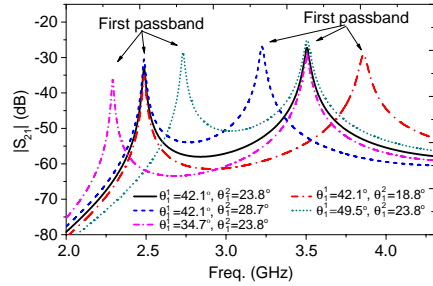
Figure 2. Simulated frequency responses under different lengths..

the second passband frequency can be tuned effectively by adjusting θ_1^2, while the center frequency of the first passband frequency keeps constant.

3. COUPLING STRUCTURE AND EXTERNAL QUALITY

Figure 3(a) shows the coupling structure of the dual-band filter, the stubs are folded properly to obtain the required coupling strength. It is designed on a substrate with dielectric $\varepsilon_r = 2.65$, thickness $h = 1\,\mathrm{mm}$, and loss tangent $\delta = 0.002$, the stubs are placed properly to obtain the required coupling strength. There are two kinds of coupled sections between the adjacent resonators, the coupling between the bottom stubs ($L_{i,i+1}^1$, G_1) and the coupling between the top stubs ($L_{i,i+1}^2$, G_2). The required bandwidths of the two passbands depend on coupling length and gap between resonators.

If f_{p1} and f_{p2} are defined to be the lower and higher resonant frequencies, respectively, the coupling coefficient can be obtained by

$$k_{ij} = \pm \frac{f_{p1}^2 - f_{p2}^2}{f_{p1}^2 + f_{p2}^2} \tag{3}$$

where k_{ij} represents the coupling coefficient between resonators i and j. Figure 3(b) shows the simulated coupling coefficient as a function of coupling length $L_{i,i+1}^1$ ($L_{i,i+1}^2 = 4.1\,\mathrm{mm}$, $G_2 = 0.8\,\mathrm{mm}$). The coupling coefficient k_1 increases with the increasing $L_{i,i+1}^1$ while k_2 keeps fixed (k_1 and k_2 denote the coupling coefficients at low resonance f_1, high resonance f_2, respectively), which means that the coupling between the top stubs only affects the second passband. In this kind of similar is the tendency of k_1, k_2 with the increasing $L_{i,i+1}^2$ ($L_{i,i+1}^1 = 5.4\,\mathrm{mm}$,

(a)

(b)

(c)
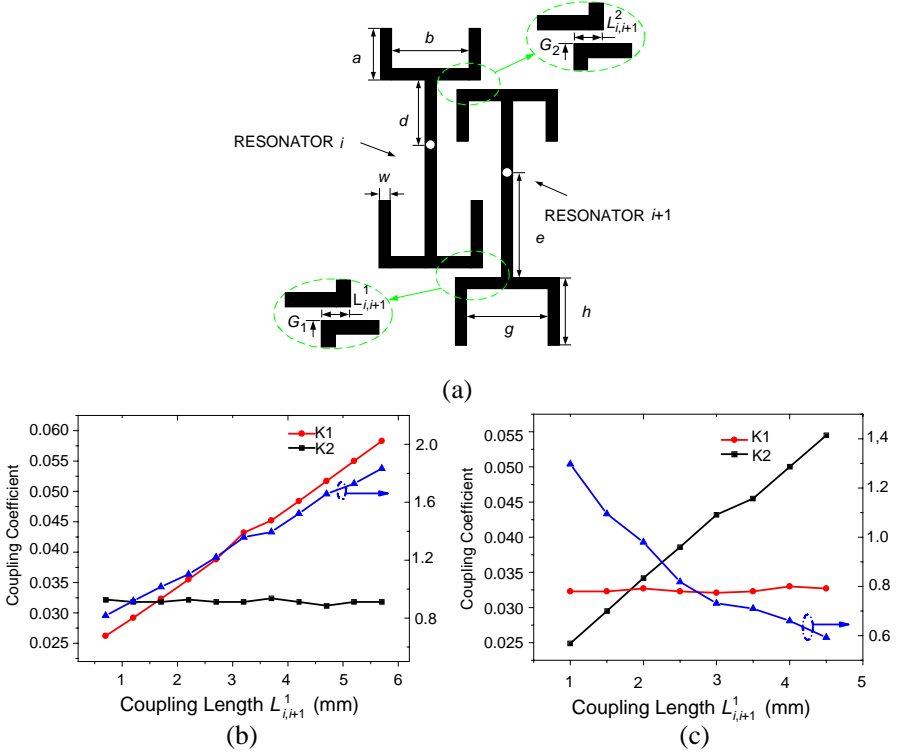
Figure 3. (a) The circuit model for calculating coupling coefficients. (b) Simulated coupling coefficients under $L_{i,i+1}^1$. (c) Simulated coupling coefficients under $L_{i,i+1}^2$.

$G_1 = 0.8\,\text{mm}$) as shown in Figure 3(c), where the coupling only affects the first passband. Since filter order and ripple level are specified and identical at the two passbands, the value of Δ_1/Δ_2 can be deduced as:

$$\frac{\Delta_1}{\Delta_2} = \frac{k_1}{k_2} \tag{4}$$

where Δ_1 and Δ_2 denote the bandwidth of the first and passbands, respectively. It should be noted that, shown in Figure 3(b), Δ_1/Δ_2 increases when $L_{i,i+1}^1$ is adjusted from 0.7 to 5.7 mm. And as shown in Figure 3(c), Δ_1/Δ_2 decreases over a wide range, i.e., from 1.3 to 0.6, while $L_{i,i+1}^2$ changes from 1 to 4.5. Thus, it is possible to build dual-band filter of $\Delta_1 \geq \Delta_2$ or $\Delta_1 < \Delta_2$ using the proposed resonator.

The coupled-line structure is employed to realize the input/output coupling because it has more degrees of freedom in the design process.

Four parameters (L_{1f}, L_{1f}, L_{3f} and L_{4f} in Figure 4(a)) can be tuned to obtain different external quality factors. For simplification, here we choose $L_{3f} = 6.1$ mm, $L_{4f} = 4.8$ mm. Thus, two independent coupled-line structures (L_{1f} and L_{2f}) are employed to realize the external quality. In other words, there are two degrees of freedom in designing the input/output coupled stages. Figure 4(b) illustrates the design graph for the filter with different L_{1f} and L_{2f}, where Q_{e1} and Q_{e2} denote the external quality factors of the first and second passbands, respectively. Proper coupled-line lengths can be selected to meet the filter specifications. Besides controlling bandwidth conveniently, this structure also can be used to design high-order dual-band BPF.
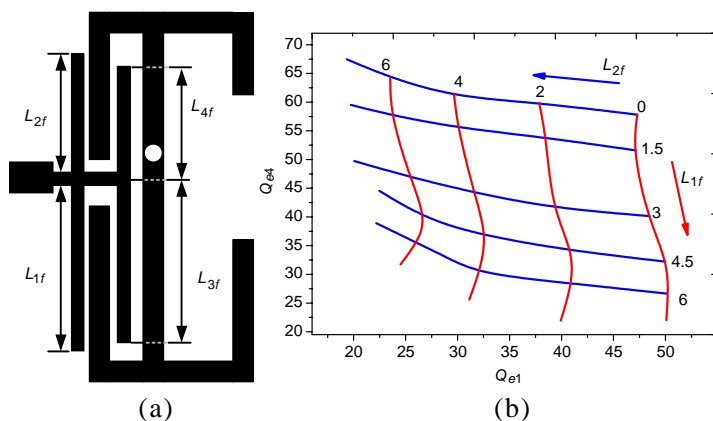
Figure 4. (a) The circuit model for calculating external quality. (b) Simulated external quality factors under different coupled-line length.

4. FILTER DESIGN AND MEASUREMENT

The design procedures of the presented dual-band filter can be summarized as follows. First of all, deduce the admittance of resonator to obtain the center frequencies of the two passbands. Then, tune the coupling between the bottom and top coupled stubs to meet the required bandwidth, properly selecting I/O coupled-line, and the required of each passband can be obtained. Finally, the optimized dual-band performance can be obtained.

From the above analysis procedure, it is obvious that both the centers and the coupling coefficients of the two passbands can be devised independently, and the passbands barely interfere each other.

To verify the effectiveness of the design, a fifth-order dual-band BPF is designed. $K_{i,i+1}^1$ denotes the coupling coefficient between the adjacent resonators at f_1, and $K_{i,i+1}^2$ denotes the coupling coefficient between the adjacent resonators at f_2. In general, $K_{12}^1 = K_{45}^1$ and $K_{23}^1 = K_{34}^1$, $K_{12}^2 = K_{45}^2$ and $K_{23}^2 = K_{34}^2$. Figure 5 shows the structure of the fifth-order filter, L_{12}^1 and L_{23}^1 (the coupling lengths between the bottom stubs) are determined by K_{12}^1 and K_{23}^1, respectively. L_{12}^2 and L_{23}^2 (the coupling lengths between the top stubs) are determined by K_{12}^2 and K_{23}^2, respectively. These coupled section parameters can be got using the same method proposed in Section 3. Simulation and measurement are carried out using Zeland IE3D software and Agilent's 8719ES network analyzer, respectively.
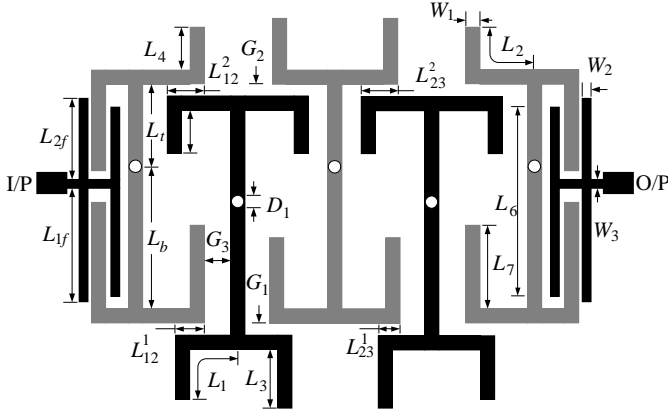
Figure 5. Layout of the fifth-order dual-band filter.

As shown in Figure 6(a), when L_{12}^1 and L_{23}^1 varies from 2.6 to 4.6 mm and from 1.2 to 3.1 mm, respectively (external quality is properly adjusted and the other parameters are fixed), the bandwidth of the first passband increases obviously (3%–4.5%), while the bandwidth of the second passband keeps fixed (3%). Besides that, the bandwidth of the second changes from 1.8% to 3.7% while the bandwidth of the first passband is constant (3.7%), which can be seen in Figure 6(b) with L_{12}^2 and L_{23}^2 varying from 2.1 to 4.1 and from 1.2 to 2.7, respectively.

A dual-band filter with a fifth-order Chebyshev frequency response and 0.1-dB ripple level is designed with the following specifications: the center frequencies of the two passbands are at 2.5 and 3.5 GHz. And the fractional bandwidths are 3.8% and 5.2%, respectively. The lumped circuit element values of the low-pass prototype filter are found
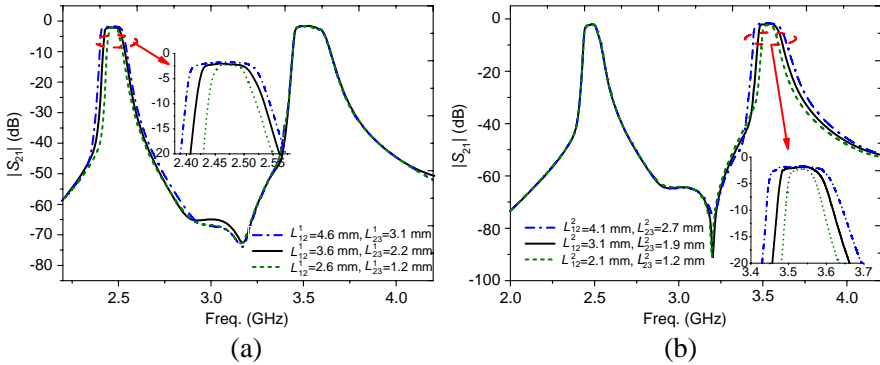
Figure 6. Simulated insertion losses under different coupling lengths (a) $L^1_{i,i+1}$. (b) $L^2_{i,i+1}$.

to be $g_0 = 1$, $g_1 = 1.1468$, $g_2 = 1.3712$, $g_3 = 1.9750$, $g_4 = 1.3712$, $g_5 = 1.1468$. The required coupling coefficients and external quality factors can then be found as

$$K_{i,i+1}|_{i=1\sim n-1} = \frac{\Delta}{\sqrt{g_i g_{i+1}}} \quad Q_e = \frac{g_i g_{i+1}}{\Delta} \quad \text{or} \quad Q_e = \frac{g_n g_{n+1}}{\Delta} \qquad (5)$$

Specifically, the coupling coefficients and external quality can be deduced according to the bandwidths $K^1_{12} = K^1_{45} = 0.030$, $K^1_{23} = K^1_{34} = 0.023$, $K^2_{12} = K^2_{45} = 0.041$, $K^3_{23} = K^3_{34} = 0.032$, $Q_{e1} = 30.2$ and $Q_{e2} = 22.1$. After an efficient optimization process, the dimensions parameters of the filter are $L_1 = 7.4$, $L_2 = 5.5$, $L_3 = 5.2$, $L_4 = 1.6$, $L_5 = 3.1$, $L_6 = 11.4$, $L_7 = 4.5$, $L_b = 8.5$, $L_t = 4.3$, $W_1 = 1.0$, $W_2 = 0.5$, $W_3 = 0.5$, $G_1 = 0.8$, $G_2 = 0.8$, $G_3 = 1.3$, $D = 0.4$, $L^1_{12} = 2.4$, $L^1_{23} = 1.1$, $L^2_{12} = 3$, $L^2_{23} = 2.4$, $L_{1f} = 5.3$, $L_{2f} = 7$ (all are in mm). Figure 7 presents a photograph of the fabricated filter. Figure 8 plots the simulated and the measured frequency responses. The measured parameters agree well with those obtained from the simulation. The measured center frequencies of this filter are at 2.49 and 3.5 GHz with the 3 dB fractional bandwidths are 3.5% and 5.1%, respectively. The minimum insertion losses are measured approximately 2.4 dB and 2.1 dB, respectively. And the measured isolation is greater than 55 dB between the desired passbands, which means that the band selectivity of this filter is very good.

Table 1 summarizes the comparison of the proposed filter with those previously reported. This dual-band general chebyshev BPF has the advantage of high order, high selectivity, compact size and independent control of passband locations. As a result, it is quite
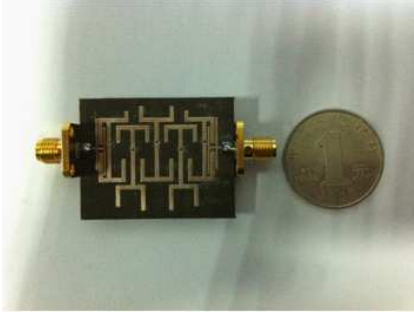
Figure 7. Photograph of the fabricated fifth-order dual-band filter.
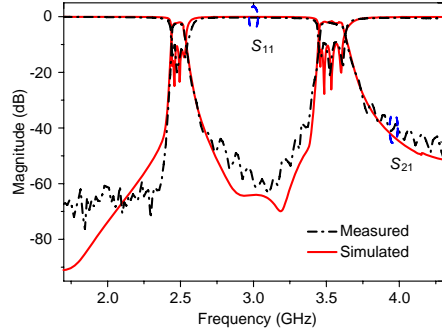
Figure 8. Simulated and measured results of the fifth-order dual-band filter.

Table 1.

Ref	1st/2nd Passband (GHz)	Order	$|S_{11}|$ (dB)	Independent Control (Both of C.F.)	Independent Control (Both of B.W.)	Size $(\lambda_g \times \lambda_g)$
[4]	2.5/5.7	2	11/22	No	No	0.09×0.04
[5]	0.9/2.4	6	14/18	No	No	0.35×0.18
[6]	2.5/5.9	5	12/12	No	No	$1.51/0.10$
[7]	2.45/5.8	4	10/10	No	No	0.72×0.15
[8]	2.4/3.5	6	8/11	No	No	0.93×0.26
Proposed Filter	2.5/3.5	5	10/10	Yes	Yes	0.41×0.34

useful for multiservice applications in future mobile communication systems.

5. CONCLUSION

In this paper, a novel combined stub-loaded resonators and its application to high-order dual-band microstrip BPF has been proposed, analyzed, and measured. The resonant frequency of the proposed resonator is flexibly controlled. Moreover, the bandwidth of each passband can be tuned conveniently by adjusting the top stubs or bottom stubs. The design methodology has been described and two passband have been implemented. As a result, with the advantage of easily controlled center frequencies and bandwidths, the proposed resonators will be widely used in practical applications.

ACKNOWLEDGMENT

REFERENCES

1. Zhang, X. Y., J. X. Chen, and Q. Xue, "Dual-band bandpass filter using stub-loaded resonators," *IEEE Microw. Wirel. Compon. Lett.*, Vol. 17, No. 8, 583–585, Aug. 2007.

2. Weng, M. H., H. W. Wu, and Y. K. Su, "Compact and low-loss dualband bandpass filter using pseudo-interdigital stepped impedance resonators for WLANs," *IEEE Microw. Wirel. Compon. Lett.*, Vol. 17, No. 3, 187–189, 2007.

3. Chu, Q. X. and F. C. Chen, "A compact dual-band bandpass filter using meandering stepped impedance resonators," *IEEE Microw. Wirel. Compon. Lett.*, Vol. 16, No. 11, 320–322, May 2008.

4. Hsu, Y., C. Y. Chen, and H. R. Chuang, "A miniaturized dual-band bandpass filter using embedded resonators," *IEEE Microw. Wirel. Compon. Lett.*, Vol. 21, No. 12, 658–660, Dec. 2011.

5. Chang, W.-S. and C.-Y. Chang, "Analytical design of microstrip short-circuit terminated stepped-impedance resonator dual-band filters," *IEEE Trans. Microw. Theory Tech.*, Vol. 59, No. 7, 1730–1739, Jul. 2011.

6. Jiang, M., L.-M. Chang, and A. Chin, "Design of dual-passband microstrip bandpass filters with multi-spurious suppression," *IEEE Microw. Wirel. Compon. Lett.*, Vol. 20, No. 4, 199–201, Apr. 2010.

7. Mondal, P. and M. K. Mandal, "Design of dual-band bandpass filters using stub-loaded open-loop resonators," *IEEE Trans. Microw. Theory Tech.*, Vol. 56, No. 1, 150–155, Jan. 2008.

8. Chen, F.-C. and Q.-X. Chu, "Novel multistub loaded resonator and its application to high-order dual-band filters," *IEEE Trans. Microw. Theory Tech.*, Vol. 58, 1551–1556, Jun. 2010.

9. Ma, D., Z. Y. Xiao, L. Xiang, X. Wu, C. Huang, and X. Kou, "Compact dual-band bandpass filter using folded SIR with two stubs for WLAN," *Progress In Electromagnetics Research*, Vol. 117, 357–364, 2011.

10. Chen, C.-H., C.-S. Shih, T.-S. Horng, and S.-M. Wu, "Very miniature dual-band and dual-mode bandpass filter designs on an integrated passive device chip," *Progress In Electromagnetics Research*, Vol. 119, 461–476, 2011.

11. Chen, C.-Y. and C.-C. Lin, "The design and fabrication of a highly compact microstrip dual-band bandpass filter," *Progress In Electromagnetics Research*, Vol. 112, 299–307, 2011.

12. Yang, R.-Y., H. Kuan, C.-Y. Hung, and C.-S. Ye, "Design of dual-band bandpass filters using a dual feeding structure and embedded uniform impedance resonators," *Progress In Electromagnetics Research*, Vol. 105, 93–102, 2010.

13. Chiou, Y.-C., P.-S. Yang, J.-T. Kuo, and C.-Y. Wu, "Transmission zero design graph for dual-mode dual-band filter with periodic stepped-impedance ring resonator," *Progress In Electromagnetics Research*, Vol. 108, 23–36, 2010.

14. Chin, K.-S. and C.-K. Lung, "Miniaturized microstrip dual-band bands-stop filters using tri-section stepped impedance resonators," *Progress In Electromagnetics Research C*, Vol. 10, 37–48, 2009.

15. Chen, F.-C. and J.-M. Qiu, "Dual-band bandpass filter with control-lable characteristics using stub-loaded resonators," *Progress In Electromagnetics Research Letters*, Vol. 28, 45–51, 2012.

16. Wang, X.-H., B.-Z. Wang, and K.-J. Chen, " Compact broadband dual-band bandpass filters using slotted ground structures," *Progress In Electromagnetics Research*, Vol 82, 151–166, 2008.

17. Xiao, J.-K. and H.-F. Huang, " New dual-band bandpass filter with compact SIR structure," *Progress In Electromagnetics Research Letters*, Vol. 18, 125–134, 2010

18. Luo, S., L. Zhu, and S. Sun, " A dual-mode dual-band bandpass filter using a single slot ring resonator," *Progress In Electromagnetics Research Letters*, Vol. 23, 173–180, 2011.

19. Vegesna, S. and M. A. Saed, "Novel compact dual-band bandpass microstrip filter," *Progress In Electromagnetics Research B*, Vol. 20, 245–262, 2010.